Supporting Information

Muñoz-Barrera and Monje-Casas 10.1073/pnas.1408017111

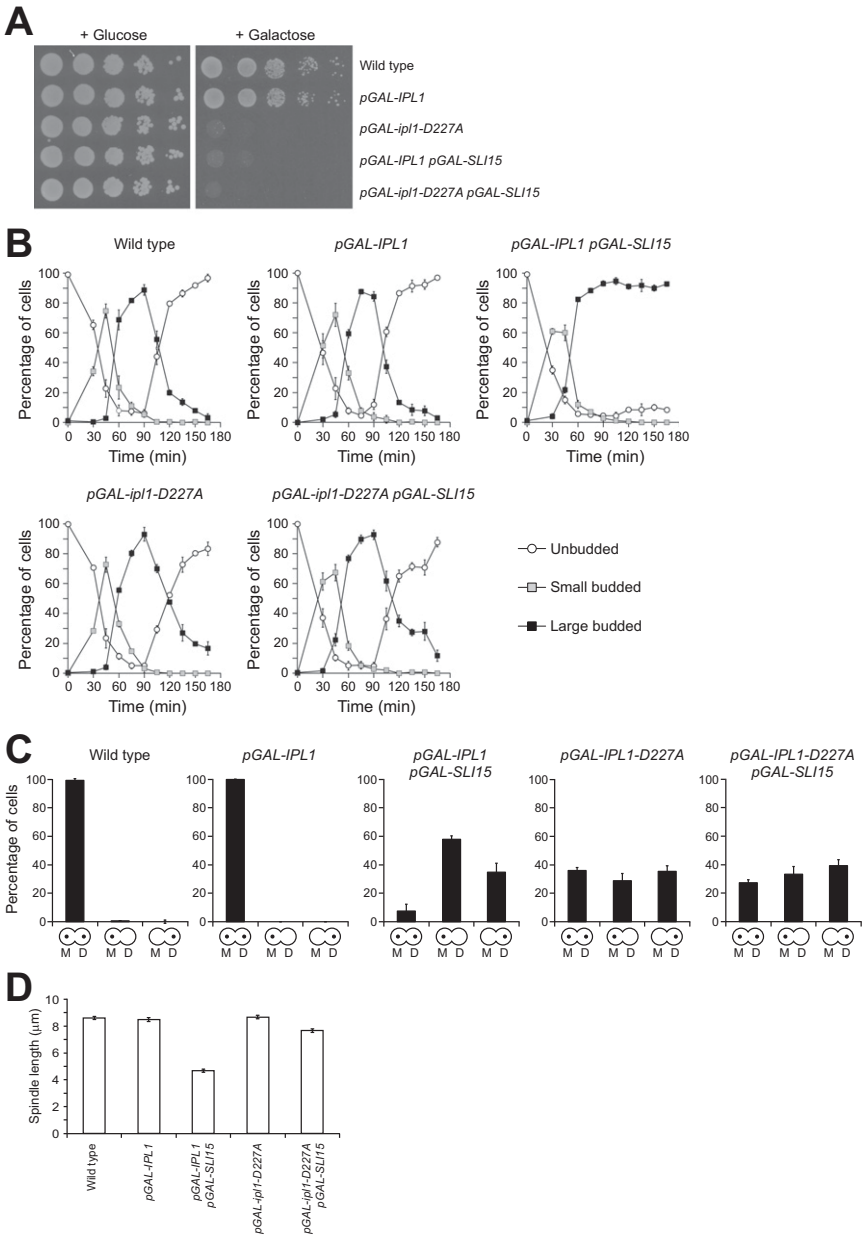

Fig. S1. Phenotypes associated with Ipl1 and Sli15 overexpression are dependent on Ipl1 kinase activity. Wild-type (F955), *pGAL-IPL1* (F256), *pGAL-IPL1 pGAL-SLI15* (F947), *pGAL-ipl1-D277A* (F2008), and *pGAL-ipl1-D277A pGAL-SLI15* (F2021) cells were grown at 25 °C in rich medium (yeast extract/peptone) with 2% raffinose (YPR). (*A*) Cell viability was determined by spotting 10-fold serial dilutions of the previous cultures grown on either yeast extract/peptone/dextrose or rich medium with 2% galactose and 2% raffinose (YPRG) plates, which then were incubated at 25 °C. (*B–D*) Cells from the cultures grown in YPR medium were arrested in G1 with 5 μg/mL α-factor and were released into fresh YPRG medium. Thirty minutes before the release, 2% galactose was added to induce transcription from *pGAL*. α-Factor was added again 75 min after release to avoid cell-cycle reentry. (*B*) Percentages of unbudded and small and large budded cells are shown for each time point. Error bars indicate SD ($n = 3$). (*C*) Analysis of chromosome segregation using CrIV-GFP dots. The graphics below the bars indicate whether sister chromatids segregated correctly [yeast cell with a dot in the mother (M) cell and a dot in the daughter (D) cell] or cosegregated either toward the mother cell (a dot only in the mother cell) or the bud (a dot only in the daughter cell). (*D*) Average maximum spindle length. Error bars indicate SEM ($n = 150$).

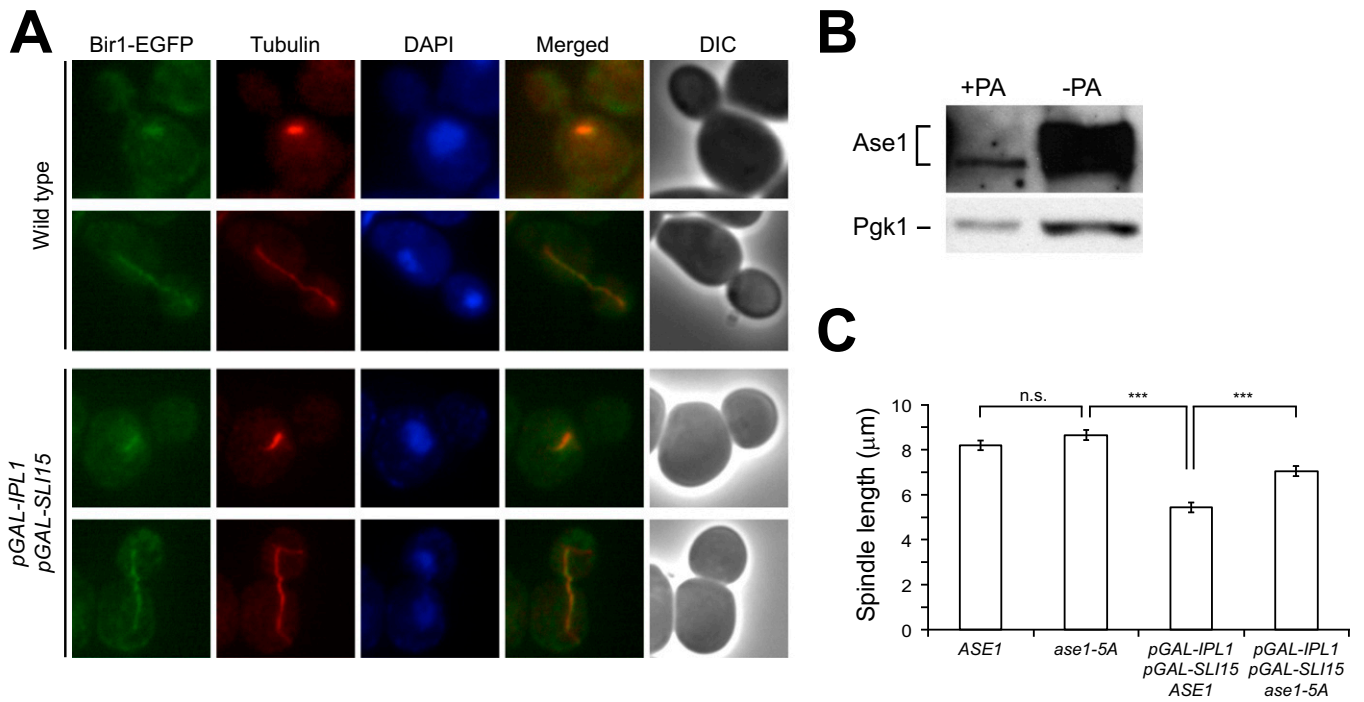

Fig. S2. Spindle instability is associated with defective Ase1 function. (*A*) Wild-type (F1357) and *pGAL-IPL1 pGAL-SLI15* (F1611) cells carrying Bir1-EGFP and Tub1-mCherry fusions were grown at 25 °C in YPR, arrested in G1 with 5 μg/mL α-factor, and released into YPRG. Thirty minutes before the release, 2% galactose was added to induce transcription from *pGAL*. Representative images showing Bir1-EGFP (green), microtubules (red), and DAPI staining (blue) and merged and differential interference contrast (DIC) images are presented. (*B*) Western blot showing Ase1-EGFP extracted from *pGAL-IPL1 pGAL-SLI15* (F1982) cells before (–PA) and after (+PA) treatment with alkaline phosphatase to demonstrate that the most slowly migrating bands are caused by phosphorylation of the protein. Pgk1 was used as a loading control. (*C*) Wild-type (F2299), *ase1-5A* (F2289), *pGAL-IPL1 pGAL-SLI15* (F2300), and *pGAL-IPL1 pGAL-SLI15 ase1-5A* (F2288) cells were allowed to enter mitosis synchronously in YPRG as in *A*. The graph shows average maximum spindle length after the release. Error bars indicate SEM ($n = 75$). Statistically significant (***$P < 0.0001$) and nonsignificant (n.s.) differences according to a two-tailed *t* test are indicated.

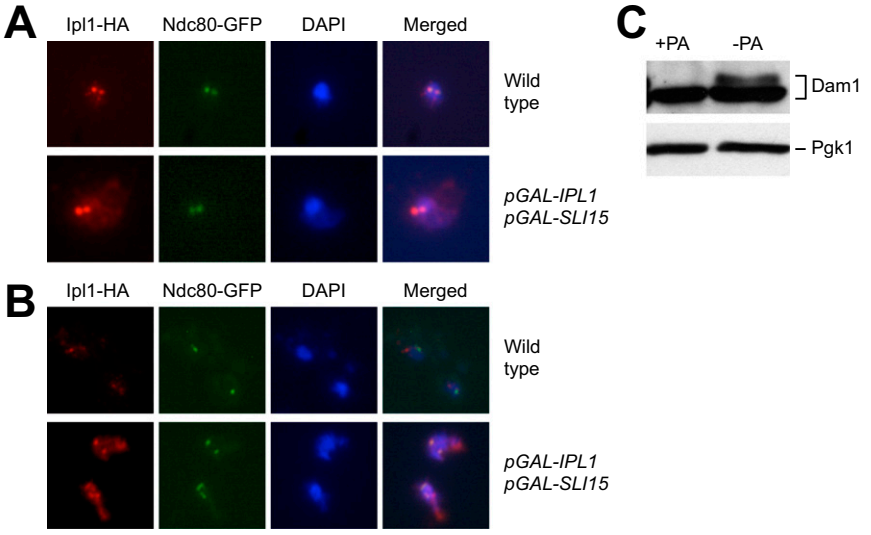

Fig. S3. Ipl1 localizes to the centromeres and hyperphosphorylates Dam1 in cells simultaneously overexpressing Ipl1 and Sli15. (*A* and *B*) Wild-type (F302) and *pGAL-IPL1 pGAL-SLI15* (F2263) cells carrying HA-tagged Ipl1 fusions and expressing Ndc80-GFP were grown in YPR at 25 °C, were arrested in G1 with 5 μg/mL α-factor, and were released into YPRG. Thirty minutes before the release, 2% galactose was added to induce transcription from *pGAL*. Representative images of chromosome spreads showing Ipl1-HA (red), Ndc80-GFP (green), and DAPI staining (blue) and a merged image are presented for metaphase cells (*A*) and after chromosome segregation (*B*). (*C*) Western blot showing Dam1-3HA extracted from *pGAL-IPL1 pGAL-SLI15* (F2274) cells before (–PA) and after (+PA) treatment with alkaline phosphatase to demonstrate that the most slowly migrating bands are caused by phosphorylation of the protein. Pgk1 was used as a loading control.

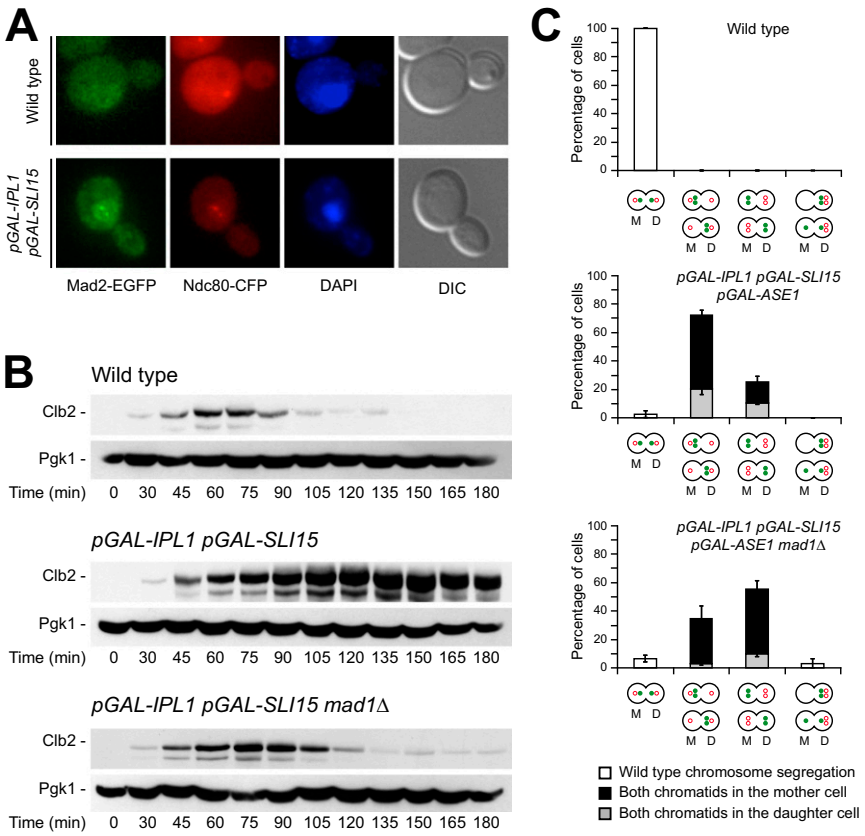

Fig. S4. Ipl1 and Sli15 overexpression leads to constitutive activation of the spindle-assembly checkpoint. (*A*) Wild-type (F217) and *pGAL-IPL1 pGAL-SLI15* (F1963) cells carrying Mad2-EGFP and Ndc80-CFP fusions were grown in YPR at 25 °C, were arrested in G1 with 5 μg/mL α-factor, and were released into YPRG medium. Thirty minutes before the release, 2% galactose was added to induce transcription from *pGAL*. α-Factor was added again 75 min after release to avoid cell-cycle reentry. Representative images showing Mad2-EGFP (green), Ndc80-CFP (red), and DAPI staining (blue) and DIC images are presented. (*B*) Wild-type (F144), *pGAL-IPL1 pGAL-SLI15* (F980), and *pGAL-IPL1 pGAL-SLI15 mad1*Δ (F1376) cells also expressing Pds1-3HA were allowed to enter mitosis synchronously in YPRG as in *A*. The Western blots show the levels of Clb2 at the indicated time points. Pgk1 was used as a loading control. (*C*) Analysis of chromosome and spindle-pole body (SPB) segregation in wild-type (F1483), *pGAL-IPL1 pGAL-SLI15 pGAL-ASE1* (F1908), and *pGAL-IPL1 pGAL-SLI15 pGAL-ASE1 mad1*Δ (F1910) cells carrying CrIV-GFP and a Spc42-mCherry fusion. Cells were allowed to enter mitosis synchronously in YPRG as in *A*. The graphics below the bars indicate the different patterns of CrIV (green closed circle) and SPB (red open circle) segregation included in each category. White bars indicate wild-type chromosome segregation. Cosegregation of sister chromatids is represented by black bars [both sisters in the mother (M) cell] or gray bars [both sisters in the daughter (D) cell].

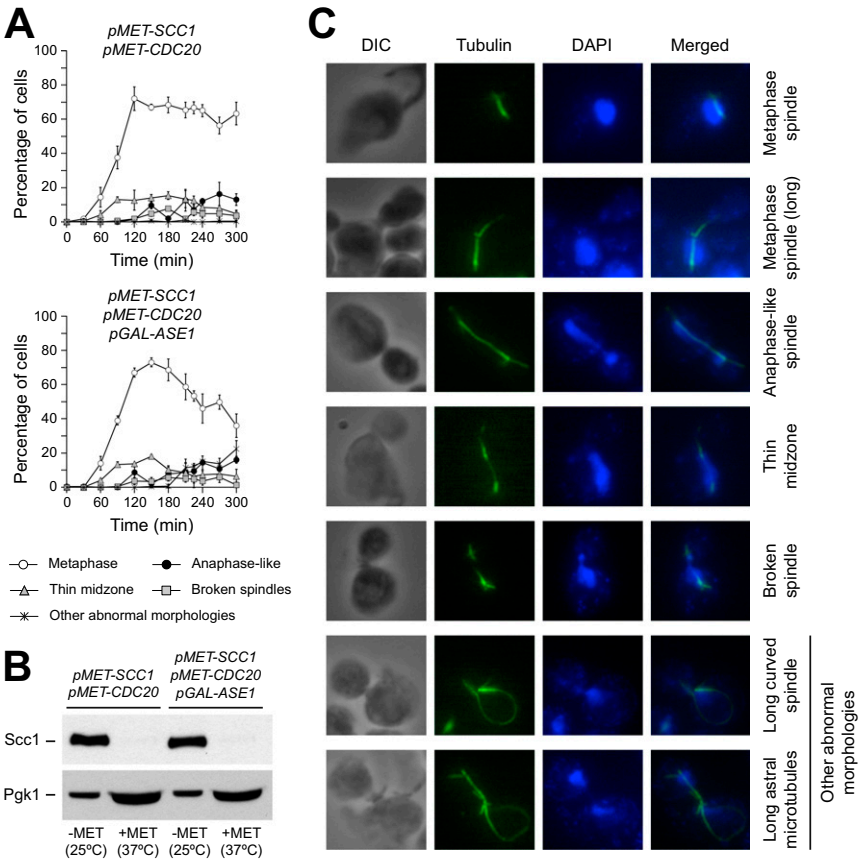

Fig. S5. Ase1 overexpression does not recover spindle instability in metaphase-arrested cells depleted of cohesin. *pMET3-SCC1-18Myc pMET3-CDC20* (F2290) and *pMET3-SCC1-18Myc pMET3-CDC20 pGAL-ASE1* (F2291) cells were grown at 25 °C in synthetic complete (SC) medium with 2% raffinose and without methionine (−MET), were arrested in G1 with 5 μg/mL α-factor, and were released into SC with 2% raffinose and 8 mM methionine (+MET) at 37 °C. Thirty minutes before the release, 8 mM methionine was added to repress transcription from *pMET3*, and cells were transferred at the restrictive temperature. Methionine was added each hour after the release to ensure an efficient transcriptional repression. Once cells reached metaphase, 2% galactose was added to the medium to induce expression from the *pGAL* promoter. (*A*) Cell-cycle progression was analyzed by spindle (tubulin) and nuclear (DAPI) morphology. Percentages of metaphase and anaphase cells and of cells carrying spindles with a thin midzone, broken spindles, or spindles with other abnormal morphologies (see *C* for examples) are shown for each time point. Error bars indicate SD ($n = 3$). (*B*) Western blot showing Scc1-18myc levels before release from α-factor (−MET, 25 °C) and at the final time point (+MET, 37 °C) to demonstrate efficient cohesin depletion. Pgk1 was used as a loading control. (*C*) Representative images of cells from the different categories established in *A*. Tubulin (green), DAPI staining (blue), and a merged and a DIC image are shown in each case.

Table S1. Strains used in this study

Strain	Relevant genotype
F496	MATa wild type
F955	MATa, *pURA3::tetR::GFP::LEU2, cenIV::tetOx448::URA3*
F256	MATa, *pURA3::tetR::GFP::LEU2, cenIV::tetOx448::URA3, trp1::pGAL-IPL1::TRP1*
F953	MATa, *pURA3::tetR::GFP::LEU2, cenIV::tetOx448::URA3, ura3::pGAL1-10-SLI15::URA3*
F1640	MATa, *pURA3::tetR::GFP::LEU2, cenIV::tetOx448::URA3, his3::pGAL-BIR1::HIS3*
F947	MATa, *pURA3::tetR::GFP::LEU2, cenIV::tetOx448::URA3, trp1::pGAL-IPL1::TRP1, ura3::pGAL1-10-SLI15::URA3*
F1642	MATa, *pURA3::tetR::GFP::LEU2, cenIV::tetOx448::URA3, ura3::pGAL1-10-SLI15::URA3, his3::pGAL-BIR1::HIS3*
F1644	MATa, *pURA3::tetR::GFP::LEU2, CenIV::tetOx448::URA3, trp1::pGAL-IPL1::TRP1, his3::pGAL-BIR1::HIS3*
F1646	MATa, *pURA3::tetR::GFP::LEU2, CenIV::tetOx448::URA3, trp1::pGAL-IPL1::TRP1, ura3::pGAL1-10-SLI15::URA3, his3::pGAL-BIR1::HIS3*
F144	MATa, *pURA3::tetR::GFP::LEU2, cenIV::tetOx448::URA3, pds1::PDS1-3HA::HIS3MX6*
F980	MATa, *pURA3::tetR::GFP::LEU2, cenIV::tetOx448::URA3, pds1::PDS1-3HA::HIS3MX6, trp1::pGAL-IPL1::TRP1, ura3::pGAL1-10-SLI15::URA3*
F1191	MATa, *pURA3::tetR::GFP::LEU2, cenIV::tetOx448::URA3, pds1::PDS1-3HA::HIS3MX6, trp1::pGAL-IPL1::TRP1*
F1196	MATa, *pURA3::tetR::GFP::LEU2, cenIV::tetOx448::URA3, pds1::PDS1-3HA::HIS3MX6, ura3::pGAL1-10-SLI15::URA3*
F1376	MATa, *pURA3::tetR::GFP::LEU2, cenIV::tetOx448::URA3, pds1::PDS1-3HA::HIS3MX6, trp1::pGAL-IPL1::TRP1, ura3::pGAL1-10-SLI15::URA3, mad1::HIS3MX6*
F1912	MATa, *pURA3::tetR::GFP::LEU2, cenIV::tetOx448::URA3, pds1::PDS1-3HA::HIS3MX6, trp1::pGAL-IPL1::TRP1, ura3::pGAL1-10-SLI15::URA3, his3::pGAL-ASE1::HIS3*
F1735	MATa, *pURA3::tetR::GFP::LEU2, CenIV::tetOx448::URA3, trp1::pGAL-IPL1::TRP1, ura3::pGAL1-10-SLI15::URA3, his3::pGAL-ASE1::HIS3*
F1753	MATa, *his3::pIPL1-IPL1::HIS3*
F1754	MATa, *trp1::pSLI15-SLI15::TRP1*
F2019	MATa, *his3::pIPL1-IPL1::HIS3, trp1::pSLI15-SLI15::TRP1*
F2008	MATa, *pURA3::tetR::GFP::LEU2, cenIV::tetOx448::URA3, trp1::pGAL-ipl1-D227A::TRP1*
F2021	MATa, *pURA3::tetR::GFP::LEU2, cenIV::tetOx448::URA3, trp1::pGAL-ipl1-D227A::TRP1, ura3::pGAL1-10-SLI15::URA3*
F1670	MATa, *pURA3::tetR::GFP::LEU2, CenIV::tetOx448::URA3, pMET-CDC20::URA3*
F1948	MATa, *pURA3::tetR::GFP::LEU2, CenIV::tetOx448::URA3, pMET-CDC20::URA3, trp1::pGAL-IPL1::TRP1, ura3::pGAL1-10-SLI15::URA3*
F1483	MATa, *spc42::SPC42-mCherry::KanMX6, pURA3::tetR::GFP::LEU2, cenIV::tetOx448::URA3*
F1417	MATa, *trp1::pGAL-IPL1::TRP1, ura3::pGAL1-10-SLI15::URA3, pURA3::tetR::GFP::LEU2, cenIV::tetOx448::URA3, spc42::SPC42-mCherry::KanMX6*
F1927	MATa, *pURA3::tetR::GFP::LEU2, CenIV::tetOx448::URA3, trp1::pGAL-IPL1::TRP1, ura3::pGAL1-10-SLI15::URA3, mad1::HIS3MX6, spc42::SPC42-mCherry::KanMX6*
F1562	MATa, *trp1::p::TRP1, ura3::pGAL1-10-SLI15::URA3, pURA3::tetR::GFP::LEU2, cenIV::tetOx448::URA3, spc42::SPC42-mCherry::KanMX6, nup159::NUP159-GFP-TRP1*
F1811	MATa, *trp1::pGAL-IPL1::TRP1, ura3::pGAL1-10-SLI15::URA3, mad1::HIS3MX6, pURA3::tetR::GFP::LEU2, cenIV::tetOx448::URA3, spc42::SPC42-mCherry::KanMX6, nup159::NUP159-GFP-TRP1*
F1845	MATa, *pURA3::tetR::GFP::LEU2, CenIV::tetOx448::URA3, trp1::pGAL-IPL1::TRP1, ura3::pGAL1-10-SLI15::URA3, mad1::HIS3MX6*
F1700	MATa, *pURA3::tetR::GFP::LEU2, CenIV::tetOx448::URA3, trp1::pGAL-IPL1::TRP1, ura3::pGAL1-10-SLI15::URA3, ahc1::His3MX6*
F1908	MATa, *pURA3::tetR::GFP::LEU2, CenIV::tetOx448::URA3, trp1::pGAL-IPL1::TRP1, ura3::pGAL1-10-SLI15::URA3, his3::pGAL-ASE1::HIS3, spc42::SPC42-mCherry::KanMX6*
F1910	MATa, *pURA3::tetR::GFP::LEU2, CenIV::tetOx448::URA3, trp1::pGAL-IPL1::TRP1, ura3::pGAL1-10-SLI15::URA3, his3::pGAL-ASE1::HIS3, mad1::HIS3MX6, spc42::SPC42-mCherry::KanMX6*
F2273	MATa, *DAM1-3HA::HIS3MX6*
F2274	MATa, *trp1::pGAL-IPL1::TRP1, ura3::pGAL1-10-SLI15::URA3, DAM1-3HA::HIS3MX6*
F217	MATa, *NDC80-CFP::TRP1, mad2::MAD2-yEGFP-HIS*
F1963	MATa, *NDC80-CFP::TRP1, trp1::pGAL-IPL1::TRP1, ura3::GAL-SLI15::URA3, mad2::MAD2-yEGFP-HIS*
F302	MATa, *NDC80-GFP::URA3, IPL1-6HA::HIS3MX6*
F2263	MATa, *NDC80-GFP::URA3, IPL1-6HA::HIS3MX6, trp1::pGAL-IPL1-3HA::TRP1, ura3::pGAL1-10-SLI15::URA3*
F1357	MATa, *ura3::pRS306-mCherry-TUB1::URA3, BIR1-yEGFP::SpHIS5*
F1611	MATa, *CenIV::tetOx448::URA3, trp1::pGAL-IPL1::TRP1, his3::pGAL1-10-SLI15::HIS3, ura3::pRS306-mCherry-TUB1::URA3, BIR1-yEGFP::SpHIS5*
F1951	MATa, *ura3::pRS306-mCherry-TUB1::URA3, ASE1-yEGFP::SpHIS5*
F1982	MATa, *trp1::pGAL-IPL1::TRP1, his3::pGAL1-10-SLI15::HIS3, ura3::pRS306-mCherry-TUB1::URA3, ASE1-yEGFP::SpHIS5*
F2299	MATa, *ase1::KanMX*, pSB152::*ASE1*::*LEU2* (CEN plasmid)
F2289	MATa, *ase1::KanMX*, pSB962::*ase1-5A*::*LEU2* (CEN plasmid)
F2300	MATa, *trp1::pGAL-IPL1::TRP1, ura3::pGAL1-10-SLI15::URA3, ase1::KanMX*, pSB152::*ASE1*::*LEU2* (CEN plasmid)
F2288	MATa, *trp1::pGAL-IPL1::TRP1, ura3::pGAL1-10-SLI15::URA3, ase1::KanMX*, pSB962::*ase1-5A*::*LEU2* (CEN plasmid)
F2290	MATa, *scc1::pMET3-SCC1-18Myc::TRP1, cdc20::pMET3-CDC20::URA3*
F2291	MATa, *scc1::pMET3-SCC1-18Myc::TRP1, cdc20::pMET3-CDC20::URA3, his3::pGAL-ASE1::HIS3*
F1570	MATa, *ura3::pAFS125-TUB1-GFP::URA3*
F1803	MATa, *trp1::pGAL-IPL1::TRP1, his3::pGAL1-10-SLI15::HIS3, ura3::pAFS125-TUB1-GFP::URA3*

All strains are W303 derivatives. Only relevant differences in the genotype with respect to the wild-type strain (F496) are shown in each case.

Table S2. Antibodies for Western blot

Protein	Primary antibody	Primary antibody dilution	Secondary antibody	Secondary antibody dilution
Pds1-3HA	Monoclonal HA.11 (Covance)	1:5,000	Anti-mouse HRP-linked (GE Healthcare)	1:10,000
Pgk1	Monoclonal anti-Pgk1 (Invitrogen)	1:20,000	Anti-mouse HRP-linked (GE Healthcare)	1:10,000
Clb2	Polyclonal anti-Clb2 (Santa Cruz Biotechnology)	1:2,000	Anti-rabbit HRP-linked (GE Healthcare)	1:10,000
H3	Polyclonal anti-histone H3 (Abcam)	1:500	Anti-rabbit HRP-linked (GE Healthcare)	1:2,000
H3S10P	Polyclonal anti-H3S10P (Santa Cruz Biotechnology.)	1:500	Anti-rabbit HRP-linked (GE Healthcare)	1:2,000
Ase1-EGFP	JL-8 Living colors monoclonal antibody (Takara Bio, Inc.)	1:1,000	Anti-mouse HRP-linked (GE Healthcare)	1:2,000
Dam1-3HA	Monoclonal HA.11 (Covance)	1:500	Anti-mouse HRP-linked (GE Healthcare)	1:1,000
Scc1-18Myc	Monoclonal 9E10 (Covance)	1:5,000	Anti-mouse HRP-linked (GE Healthcare)	1:10,000

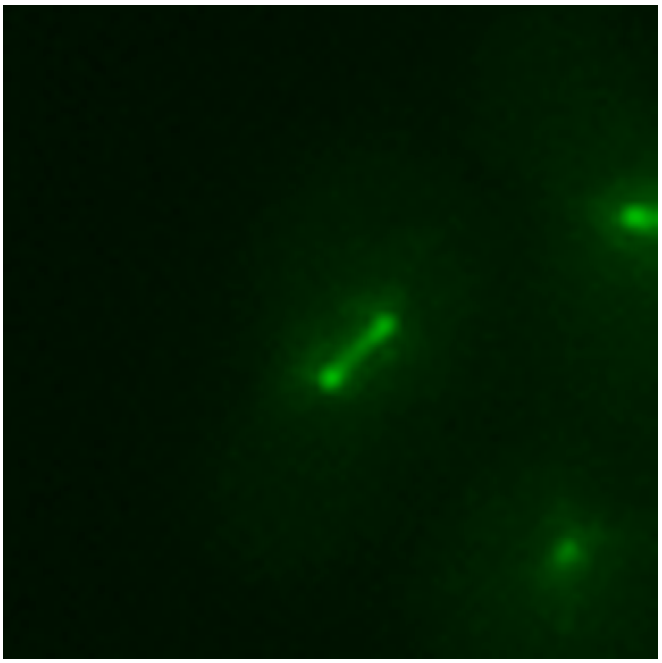

Movie S1. Spindle elongation in wild-type cells. Spindle elongation in a wild-type cell (F1570) carrying a Tub1-GFP fusion and growing in YPRG medium, as determined by time-lapse microscopy. Each time point was taken 2 min after the previous one and represents the maximum projection of a series of seven 0.78-μm–spaced *z* sections.

Movie S1

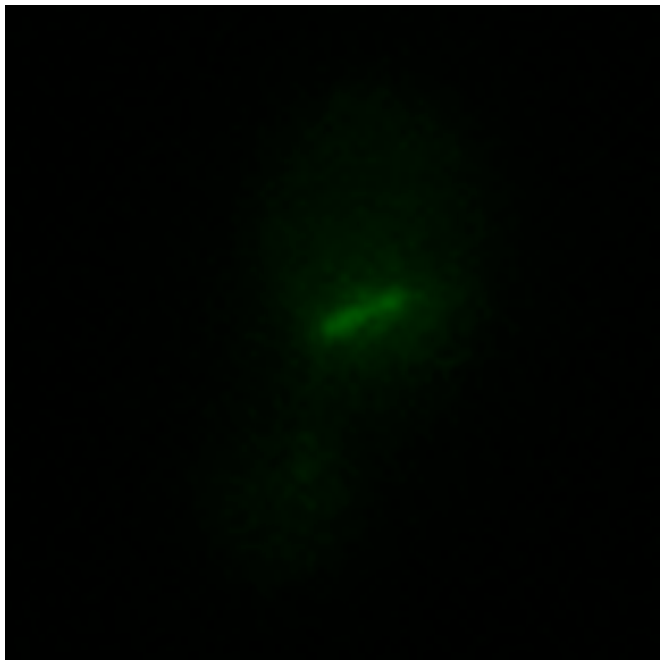

Movie S2. Spindle elongation in cells overexpressing Ipl1 and Sli15. Spindle elongation in a *pGAL-IPL1 pGAL-SLI15* cell (F1803) carrying a Tub1-GFP fusion and growing in YPRG medium, as determined by time-lapse microscopy. Each time point was taken 2 min after the previous one and represents the maximum projection of a series of seven 0.78-μm–spaced *z* sections.

Movie S2